# Hurdles to organic quinone flow cells. Electrode pasivation by quinone reduction in acetonitrile Li electrolytes

D. Rueda-García, D.P.Dubal, F. Hugenin and P.Gómez-Romero*,

Catalan Institute of Nanoscience and Nanotechnology (ICN2), CSIC and The Barcelona Institute of Science and Technology, Campus UAB, Bellaterra, 08193 Barcelona, Spain

* pedro.gomez@icn2.cat

## Abstract

The uses of quinones in Redox Flow Batteries (RFBs) has been mainly circumscribed to aqueous solutions (of derivatives with polar groups) despite a larger solubility and wider electrochemical window provided by organic media.

The redox mechanism of quinones in protic media is simpler and better known than in aprotic media, where radical species are involved.

This paper reports the behaviour of methyl-p-benzoquinone (MBQ) under electrochemical reduction conditions in a $LiClO_4$ – $CH_3CN$ electrolyte and various working electrodes. We detected the reversible generation of a bright green coating on the working electrode and the subsequent formation of a polymer (the nature of which depends on the presence or absence of oxygen). These coatings prevent the regular redox process of methyl-p-benzoquinone from taking place on the surface of the electrode and is generated regardless of the electrode material used or the presence of $O_2$ in solution. In addition to MBQ, the green passivating layer was also found for less sterically hindered quinones such as p-benzoquinone or 1,4-naphthoquinone, but not for anthraquinone. We have also shown the central role of $Li^+$ in the formation of this green layer. This work provides important guidelines for the final use of quinones in RFBs with organic electrolytes

## 1. Introduction

Quinones are the perfect example of reversible redox organic molecules. They are key pieces in natural and synthetic chemistry, from biological processes such as the mitochondrial ATP synthesis or the photosynthetic reaction center to their use as active materials in energy storage applications.[1] In both cases their effectiveness rests on their well-known reversible aqueous electrochemistry with good kinetics and a high electrochemical equivalent (two electrons per molecule of quinone).

In the field of energy storage quinones have been increasingly studied as active molecular materials for redox flow batteries (RFBs) and they count with all the characteristics necessary to conform the next generation of this type of cells. On the other hand, quinones have most frequently been used in aqueous solutions for this type of applications[2,3]. This results quite paradoxical since these organic molecules are most soluble in a variety of organic solvents rather than in water. As a matter of fact, the extended use of anthraquinone in aqueous solutions requires the sulfonation of the aromatic moiety. Thus, a plausible approach would be to explore the use of quinones in organic electrolytes as active fluid materials for RFBs. In our group have worked along that direction but have found several hurdles which we report here.

Two distinct mechanisms for the reduction of quinones have been proposed depending on the medium. For protic media the redox reactions take place in a single step involving the transference of two electrons. In this case the nature of intermediate species depends on the pH[4]. In aprotic media the redox mechanism involves two one-electron steps with a radical being generated in the first step[1,4,5], and with a second process that usually is not completely reversible.

In aprotic media, the addition of a proton source (Bronsted acid) results in an intermediate situation[4,6,7] with hydrogen-bond formation leading to a redox mechanism similar to that in protic media[8–10].

In any event, the behaviour of quinones in aprotic media is quite varied and complex because it depends on the polarity of the solvent, the support electrolyte, the quinone structure and, as explained above, the presence of protons in the media. Furthermore, the redox chemistry of quinones in aprotic media involves several possible intermediate adducts formed through weak interactions between two quinone molecules. These adducts could be anionic ($[QQ]^{2-}$, $[QQ]^{-}$ ) or radical species ($[QQ]^{\bullet}$)[6,11–13] that modify the mechanism leading to an irregular reversibility of the second redox process. The variable redox behaviour of quinones with solvent polarity[14,15] is due to the selective stabilization of some of these adduct species in different solvents. Similarly, the support electrolyte modulates the redox mechanism due to the interaction between the electrolyte cation and the different quinone anions[13–17].

Other important issue of the redox chemistry of quinones in aprotic media is a distinct trend to undergo dimerization. Indeed, the radical generated in the first redox process can react with a neutral quinone molecule, a quinone-anion or other radical leading to dimer generation[18–21]. Finally we should mention the formation of polymers as another characteristic feature of quinone electrochemistry in aprotic media. The resulting polymers can be grown as thin films on the electrode surface, [22–24] and can present conductivity and reversible redox processes, thus making them potentially useful as catalysts or electrodes. A common approach to foster these polymerization processes is the use of quinones with amino or carboxylic acid groups. For example, poly-1,5-diaminoanthraquinone is one of the most frequently studied quinone polymers as a thin film supercapacitor electrode[25–27], but it has also been studied as electrocatalyst for $O_2$ reduction[28,29].

A vast number of articles have been published on the electrochemistry of quinones. Yet, a substantial majority of them dealt with aqueous media, where the redox mechanism is better understood. As we have just discussed, the chemistry and electrochemistry of quinones in organic media is more difficult to predict, but precisely because of that it should deserve more attention.

In this work we report a detailed study of a specific combination of quinone (methyl-p-benzoquinone (MBQ)), solvent ($CH_3CN$) and electrolyte ($LiClO_4$). Acetonitrile was selected for this study due to its large dielectric constant, 38, and low viscosity, 0.34 mPa·s, together with a wide electrochemical stability window. Also we decided to work with a Li electrolyte to its widespread use and good performance in redox process applied to energy storage. Under our experimental conditions MBQ only shows a couple of redox peaks and the reversibility of its redox process depends on the concentration of $LiClO_4$, with best results for larger concentrations of $LiClO_4$. These facts made us consider the hypothesis that $Li^+$ could induce a behaviour similar to that of protons in the redox mechanism of MBQ.

The work reported here was carried on in order to confirm this hypothesis and understand the corresponding redox mechanisms. On the other hand, during the electrochemical reduction of MBQ a green layer was systematically generated onto the working electrode (regardless of the working electrode used and the presence of $O_2$ in solution). We have proven and show here how this layer prevents the MBQ redox processes from taking place, and how it can lead to a quinone polymerization process which can be reversed by the application of a positive overpotential. Similar behaviour was observed for p-benzoquinone and 1,4-naphthoquinone but not for anthraquinone.

## 2. Experimental Section

Reagents from Sigma Aldrich: 1,4-naphthoquinone (97%), acetonitrile (≥99.9%), anthraquinone (97%), lithium perchlorate (>95%), methyl-p-benzoquinone "MBQ" (98%), p-benzoquinone (98%), tetraethyammonium tetrafluoroborate (99%).

A VMP3 potentiostat-galvanostat from BioLogic with the EC-Lab 10.44 version was used for the electrochemical measures. Glassy carbon disk of 3 mm diameter from CH Instruments Inc. (CHI 104) electrode and a Pt sheet were used as working (WE) electrode, a Pt mesh as a counter electrode (CE). We used a non-aqueous reference electrode (RE) $Ag/Ag^+$ from BAS Inc. (013394), based on a solution of 0.1 M tetrabutylammonium perchlorate (TBAP) and 0.01 M $AgNO_3$ in $CH_3CN$.

Cyclic Voltammetry and Potentiostatic Electrochemical Impedance Spectroscopy (PEIS) experiments were performance with the same 3 electrodes configuration, working frequencies were from 10 kHz to 100 mHz. Before each PEIS measure was made a chronoamperometry experiment of 10 minutes to obtain a current with low variation front time, was not possible apply a longer time in the chronoamperometry experiments by large volatility of the solution to obtain a better constant current, a longer time would promote a significant concentration difference between the experiments. Also before each experiment the glassy carbon electrode was polished.

UV-Vis spectroscopy VS potential applied on the working electrode experiments were done with an Autolab PGSTAT30 potentiostat/galvanostat. Chromogenic analysis was performed concomitant with the electrochemical experiments using a USB4000 spectrophotometer (Ocean Optics Inc) equipped with an LS1 tungsten halogen light source and fiber optic cables with a diameter of 600 µm.

## 3. Results and Discussion

Cyclic voltammetry experiments of MBQ solutions in $LiClO_4$ / $CH_3CN$ electrolytes showed an apparently single (or two unresolved) redox couple process in contrast to the typical behavior of quinones in aprotic solvents, which show two well-resolved processes. Figure 1 compares CVs for the same MBQ in two different acetonitrile electrolytes, showing the remarkable difference between $LiClO_4$ and tetraethylammonium tetrafluoroborate (TEATFB).

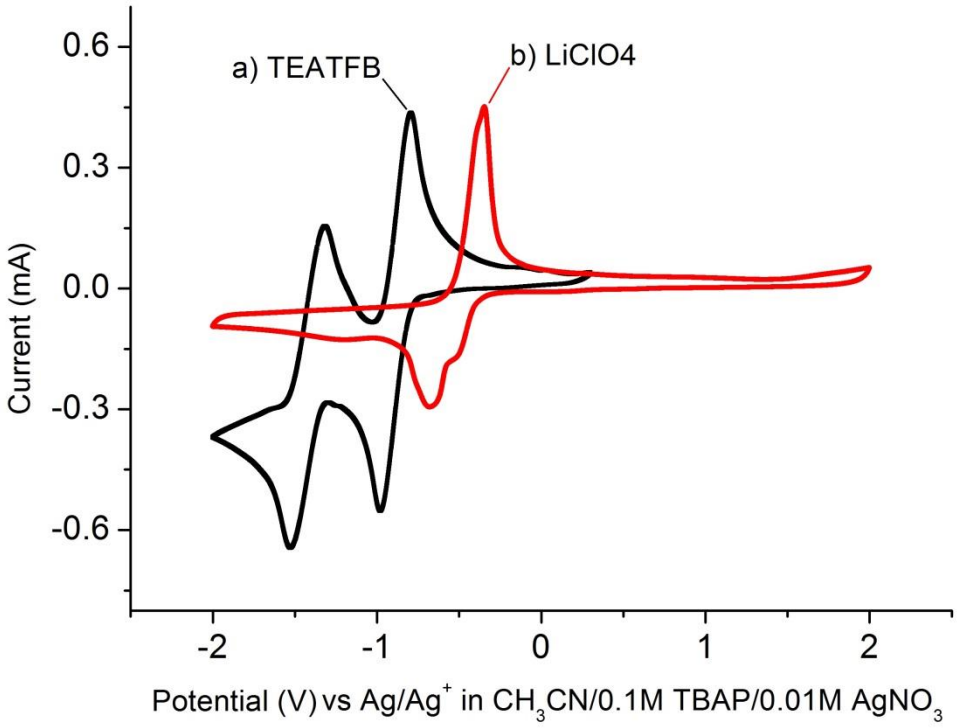


Fig. 1. Cyclic voltammetry with glassy carbon WE at 100 mV $s^{-1}$ of 0.01M MBQ solution in $CH_3CN$, a) 1.5M $LiClO_4$ b) 1M TEATFB

Another remarkable difference between the electrochemistry of MBQ in TEATFB and in LiClO4 electrolytes is the generation of a bright green coating upon application of negative potentials associated to the reduction of MBQ. This green coating, which will be discussed in detail below (Figure 3d) is formed regardless of the working electrode, scan rate and electrolyte concentration used. Indeed, we found it in every experiment we run.

But before dealing with this conspicuous green layer, we need to discuss another important element of this work, namely, the effect of $Li^+$ concentration on the electrochemistry of MBQ. Figure 2 shows CVs of MBQ with various concentrations of $LiClO_4$ in acetonitrile electrolytes recorded at 100 mV $s^{-1}$. The separation between oxidation and reduction peaks of MBQ (indicative of the reversibility of the redox potentials) depends on the concentration of $LiClO_4$. Low concentration of salt leads to a wide and weaker oxidation peak which is shifted to higher potential, indicating a poorly reversible oxidation process (figure 2a). As the concentration of $LiClO_4$ is increased the oxidation peak gets better resolved and shifts to lower potentials (figure 2b). Thus, the larger concentration of $LiClO_4$ used led to the minimum distance between oxidation and reduction peaks by a displacement of the oxidation peak to more negative potentials (figure 2c).

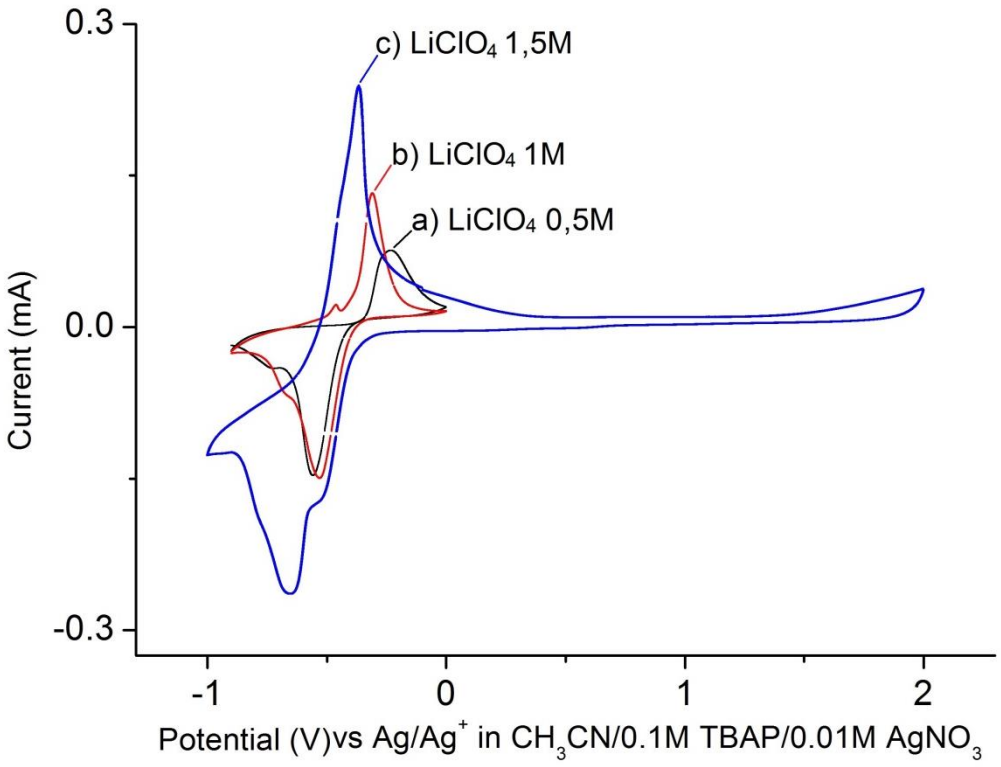


Fig. 2 .Cyclic voltammetry with glassy carbon WE at 100 mV $s^{-1}$ of 0.01M MBQ solution in $CH_3CN$, a) 0.5M $LiClO_4$ b) 1M $LiClO_4$ c) 1.5M $LiClO_4$.

Thus, an increase of the $LiClO_4$ concentration increases the reversibility of the redox process of MBQ. This indicates that $Li^+$ ions stabilize the MBQ anions generated by the reduction process. Accordingly, any possible irreversible reaction which MBQ anions could undergo for low lithium concentrations are minimized with high lithium concentrations, thus allowing the generation of a reduced product able to be reoxidized. Furthermore, it should be noted that the oxidation process is composed of two individual steps, as indicated by the shoulder in the oxidation peak in figure 2c. That indicates that the redox of MBQ in our conditions takes place in two steps at very close potentials, implying the presence of a radical species in the MBQ redox mechanism.

Cyclic voltammetry experiments at lower scan rates (10 mV $s^{-1}$) show a decrease of the intensity in each cycle (figures 3a-c) with a faster collapse for the oxidation peak. That behaviour is associated to the very conspicuous and fast generation of a green layer coating the WE. That coating was generated at negative potentials corresponding to the reduction of MBQ and was formed regardless of $Li^+$ concentration, scan rate or materials used as WE (figure 3d), in our case, Pt, Au Ni and Cu, as well as various carbon electrodes, including glassy carbon. Remarkably, it was possible to remove this coating, produced by the reduction of the MBQ, with the application of a positive overpotential, but this reoxidation is a slower process than the reductive coating process as is proved by the experiments at 10 mV $s^{-1}$.

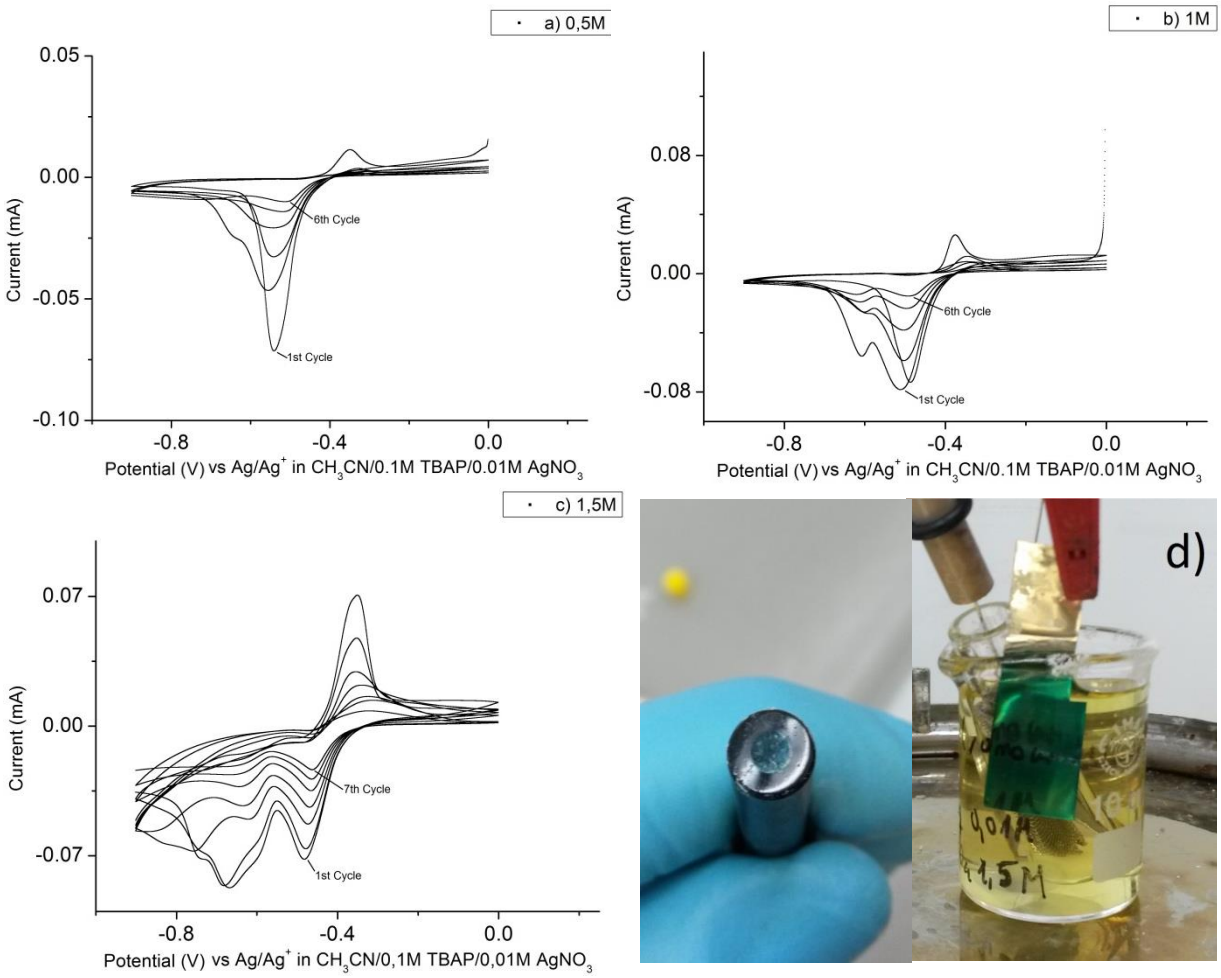


Fig. 3. Cyclic voltammetry with glassy carbon WE at 10mV $s^{-1}$ of 0.01M MBQ solution in $CH_3CN$, a) 0.5M $LiClO_4$ b) 1M $LiClO_4$ c) 1.5M $LiClO_4$, d) Glassy carbon and Pt sheet as WE covered by the MBQ reduction.

The electrode passivation at low scan rate indicate that the reduction process is faster than oxidation. The progressive collapse of CV waves upon cycling indicates that the coating generated on the surface of the electrode by the reduction process increases in each cycle, with the resistance of the electrode increasing at the same time. This is consistent with a polymerization process taking place on the surface of the electrode. This electropolymerization process is clearly associated to the reduction peak appearing at the more negative potentials on the CVs (figure 2c). That peak is much better resolved in the CV of figure 2c than in 2a,b. The reason is that the former CV was run up to a large positive potential, thus allowing enough time for the green coating to dissolve after each cycle (a dissolution which was ascertained by visual inspection). This resulted in the polymerization process to start anew in each cycle leading to a well-defined electropolymerization peak. This hypothesis is supported by results at low scan rate, figures 3a-c, where the most negative peaks disappear faster than the other reduction peaks upon cycling.

Impedance studies corroborate the mechanism proposed by the CV experiments. The impedance experiments were performance at five different potentials in order to study the different processes taking place on the electrode

surface. Figure 4a shows Nyquist plots recorded at each of those potentials, and figure 4b presents the corresponding polarization curve. A glassy carbon disk electrode was used as WE in all the PEIS experiments.

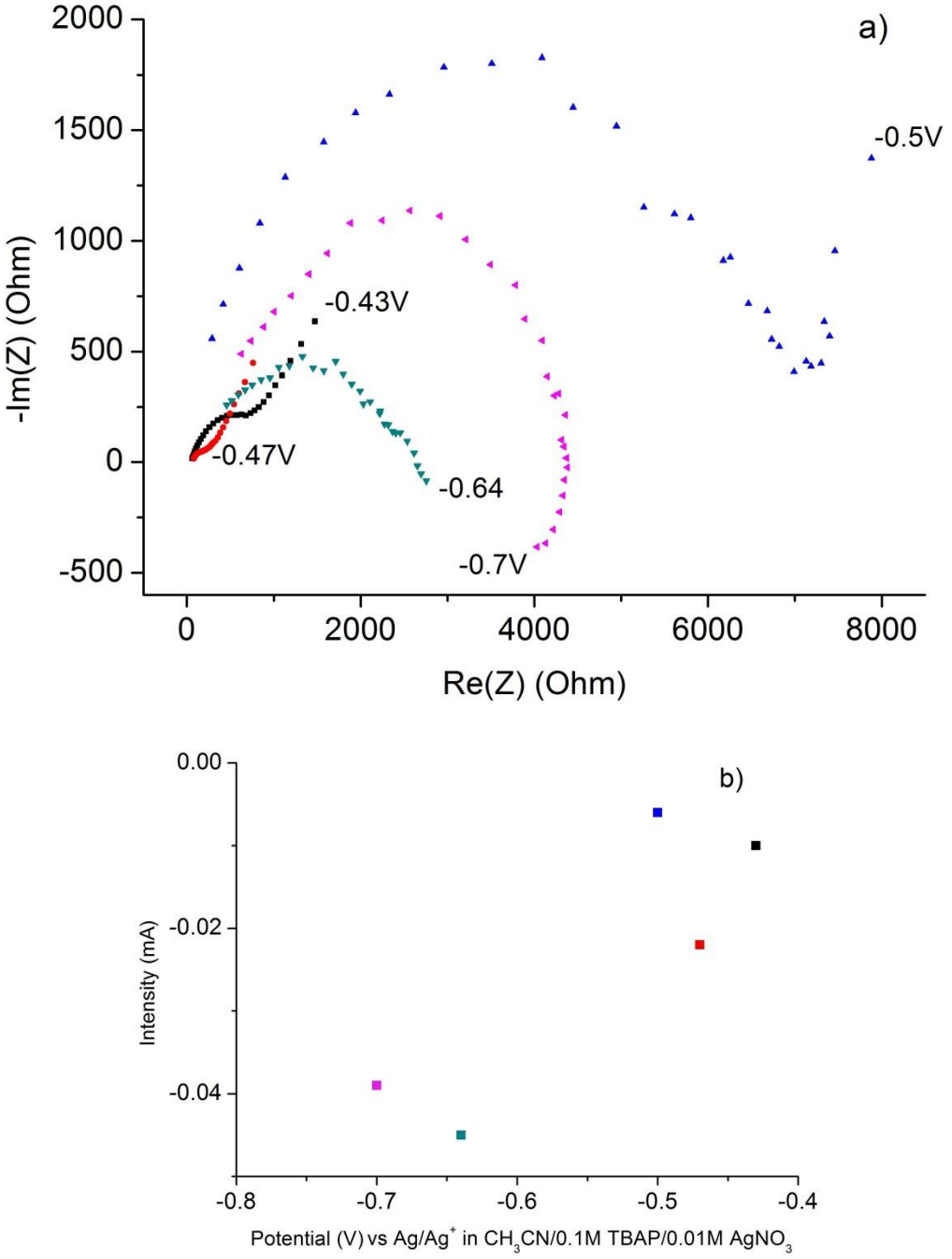


Fig. 4. a) Nyquist plot of the different potentials applied, b) Polarization curve.

The first point was recorded at -0.43V, a potential less negative than the reduction peak of MBQ. The corresponding series in the Nyquist plot shows the typical behaviour for a simple electrochemical redox process, a semicircle at high frequencies due to the electron transfer and a 45º straight line at low frequencies

due to mass transport. The second point (-0.47V) corresponds to the first reduction peak, corresponding to the reversible reduction of MBQ. It also shows the behaviour of a simple electrochemical redox process. In this case the resistance associated to electron transfer decreases and the current increases due to the application of a larger overpotential allowing for a maximum velocity for electron transfer between MBQ and the electrode. It should be noted that no green coating was detected on the electrode surface after these two PEIS experiments.

The third point (-0.5V) is located between the peak of reversible reduction of MBQ and the second reduction peak that we assign to a polymerization process. At this potential the resistance associated with the electron transfer is the largest of all the potentials studied and, correspondingly, the current is the lowest. The shape in the Nyquist plot changes radically with respect to the two previous cases. The semicircle can be considered completed but it is irregular and is followed by a line with larger slope than in the two previous cases at less negative potentials discussed above. The large semicircle clearly indicates that the resistance for the redox process of MBQ increases substantially. On the other hand, the large slope after the semicircle indicates a capacitive behaviour which is compatible with the adsorption of MBQ on the electrode and not diffusing to the solution. Indeed, at the end of this experiment, the green coating was apparent on the surface of the electrode, thus confirming the MBQ adsorption. All these observations conform to a picture in which the application of a potential negative enough (-0.5V), leads to a faster reduction of MBQ, which results in an increased concentration of the reduced product on the electrode surface; a concentration high enough to lead to the formation of the green coating, which in turn blocks the surface to the reduction of the remaining MBQ in solution. This blocking barrier (not yet an insoluble polymer) is responsible for the largest resistance observed and the very small current associated.

The fourth point (-0.64V) is integrated in the second reduction peak. As mentioned before, this potential was associated to the growth of a blocking polymer leading to the collapse of intensity of CVs at low scan rate (Fig. 3). At this potential the shape of the Nyquist plot is similar to that of the third point (at -0.5V) but the resistance associated to the electron transfer is much smaller (Fig 4 a). Furthermore, the series for this fourth point shows negative values of the imaginary component of impedance for the last three points. Finally, this point presents the largest intensity value despite having a larger resistance than the first and second points. This large intensity confirms that an electropolymerization process is effectively taking place. The larger resistance of the electrode compared to the two first points indicates that it is covered, so the process involved at this potential takes place on the coating not on the electrode surface and the product resulting from that process is characterized by a lower resistance than the (green) coating produced at the third voltage point. This means that a new product is generated on the electrode surface. It should be noted that after this experiment the electrode was coated with a darker material, which was more difficult to remove from the electrode than the green coating formed

at the third potential point. Thus, the green coating grown at -0.5V could be easily removed by dissolution in acetonitrile whereas the darker coating of this fourth point (-0.64V) could not be dissolved in a similar way and needed scratching the electrode surface to be removed.

The fifth point (-0.7V) was fixed after the second reduction point. As it could be expected for the continuing growth of the polymer coating, the intensity decreases and the resistance increases with respect to the values found for the fourth point. The shape on the Nyquist plot is still not well defined but shows a semicircle on the negative imaginary impedance zone that indicates an inductance due to the larger thickness of the coating on the working electrode. To a lesser extent this behaviour can also be appreciated on the fourth point (the last three points extending to the negative zone of the imaginary impedance component).

All the experiments described so far were carried out in air. In order to establish the possible involvement of oxygen in the formation of the described coatings, a series of parallel experiments in deaerated electrolytes under argon were carried out. These experiments were necessary since it is well known that reduced quinone species and polymers can reduce oxygen[30].

Figure 4 shows the CV of a solution of MBQ in deaerated acetonitrile and under Ar flow (5a) and in air, as above (5b). Despite the obvious similarities we note that the solution without oxygen, 4a, shows more intense and better resolved oxidation peaks. This can be explained by a larger concentration of reduced species in each cycle thanks to the absence of dissolved oxygen, which could otherwise oxidize part of the reduced MBQ.

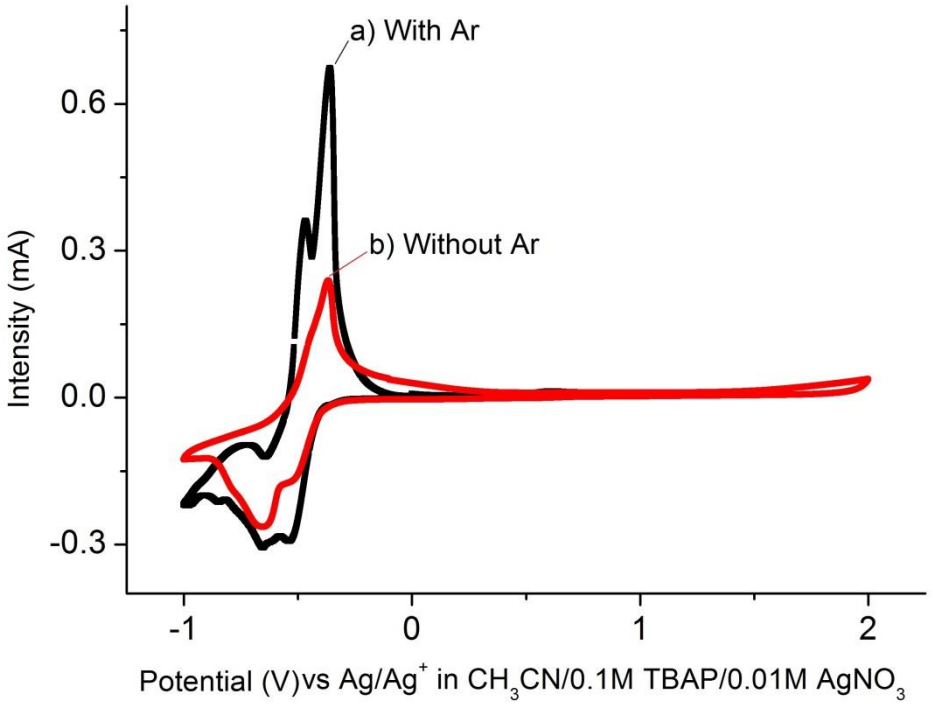

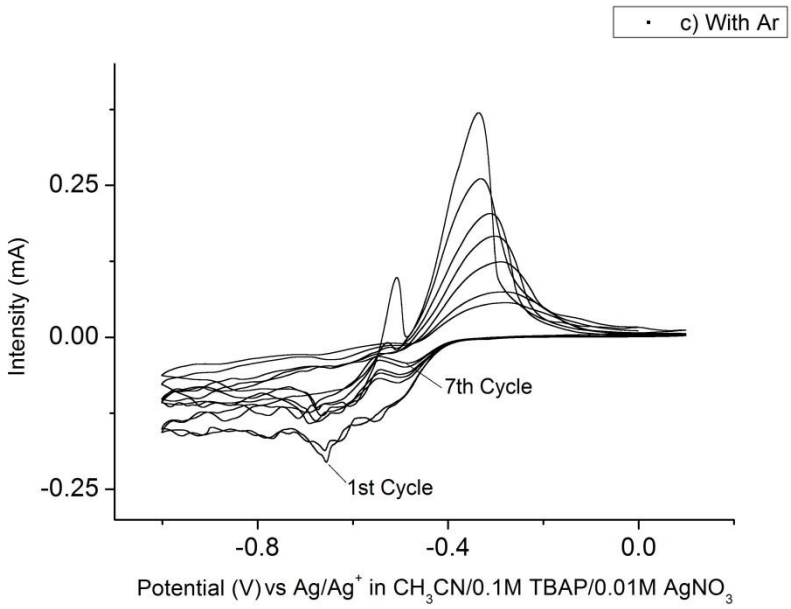


Fig. 5. Cyclic voltammetry with glassy carbon WE at 100 mV $s^{-1}$ of 0.01M MBQ, 1.5M $LiClO_4$ solution in $CH_3CN$, a) with Ar flux, b) at ambient conditions, c) at 10 mV $s^{-1}$ with Ar flux.

On the other hand, all redox peaks appear at the same potentials. And, most importantly, the green layer that was formed under air is also formed in the absence of air. Here, again, the green coating is formed on the electrode surface at negative overpotentials, and it forms much faster that it dissolves. Thus, both with and without oxygen, the green coating quickly appears, even within the timescale of a fast CV, but it needs longer times to disappear at positive potentials. Also, both with and without oxygen, the green coating passivates the electrode surface thus blocking the reversible redox process of MBQ. This can be ascertained from figure 5c, where several cycles were recorded at low scan rate. The peak at ca. -0.35 V, corresponding to the reversible oxidation of MBQ, gets collapsed upon cycling due to the accumulation of the green coating, similarly to what happened in air (figure 3c).

So the generation of the green layer is a process independent of the presence of oxygen in solution. However this will not be so for the ensuing processes following further reduction of the green layer, as we will show below. The first hint towards this conclusion comes from the very complex pattern systematically recorded on the CVs at negative overpotentials. Indeed, all Ar-deaerated CVs showed an apparently noisy signal after the negative redox peak, below ca. -0.6V (figure 5c). Our first hypothesis of an instrumental artefact was ruled out by the systematic reproducibility of these apparently irreproducible traces, characterized by a chaotic component. The chaotic nature of this (these) reduction process(es) was confirmed repeatedly. Figure S1 shows one experiment intended to probe the extent of this behaviour in a wide potential range. Indeed, the aleatory appearance of the trace goes down to -2.0 V in contrast with the behaviour in air.

Complex Impedance measurements were also performed for this oxygen-free series at voltages similar to the series run in air. Thus, figure 6 collects the corresponding Nyquist plots and polarization curve for this series, which show a different behaviour under Ar, even at the potential corresponding to the first redox peak (-0.5V), thus confirming the dependence of this process on the presence of oxygen in solution.

For the first potential point (-0.495), placed right before the first reduction peak, PEIS results under Ar show a simple electrochemical redox process as the experiment in air. And, as in air, with no signal of the green coating. In the second potential point (-0.536V), which corresponds to the first reduction peak, there is already inductive behaviour just after the formation of the green coating on the working electrode surface. In the experiment with air there was no green layer generated at this point, which can be explained by the presence of $O_2$ lowering the concentration of reduced MBQ. That is also the reason for the different trend observed for the first three points of the polarization curve in Ar versus air: the coverage process starts before reaching the potential of the peak for the reversible MBQ reduction.

The third potential point (-0.6V) is located between the two reduction peaks. In this case the impedance shows a capacitive behaviour (high slope line) and the working electrode gets the green coating layer. This different behaviour with respect to the experiments in air confirms that the polymerization mechanism depends on the presence of $O_2$. The fourth potential point (-0.66V) corresponds to the second reduction peak, the Nyquist plot shows a complete semicircle with a very low resistance followed by a straight line with a large slope. That may indicate that a redox process takes place but not involving diffusion of molecular species to the electrode and with the product generated on the electrode still acting as a capacitor. Again that behaviour is completely different from that observed in the solution with air, where the resistance was reduced in the second redox peak potential but never with a smaller value than for the first and second points. The large current and low resistance at this point confirm that there is a very favoured process, but despite being at a very similar potential to the second reduction peak in the experiments with $O_2$ is not the same process.

Finally, the last point (-1.0V) shows large resistance in the Nyquist plot and low current values, confirming the growth of a passivating product on the electrode.

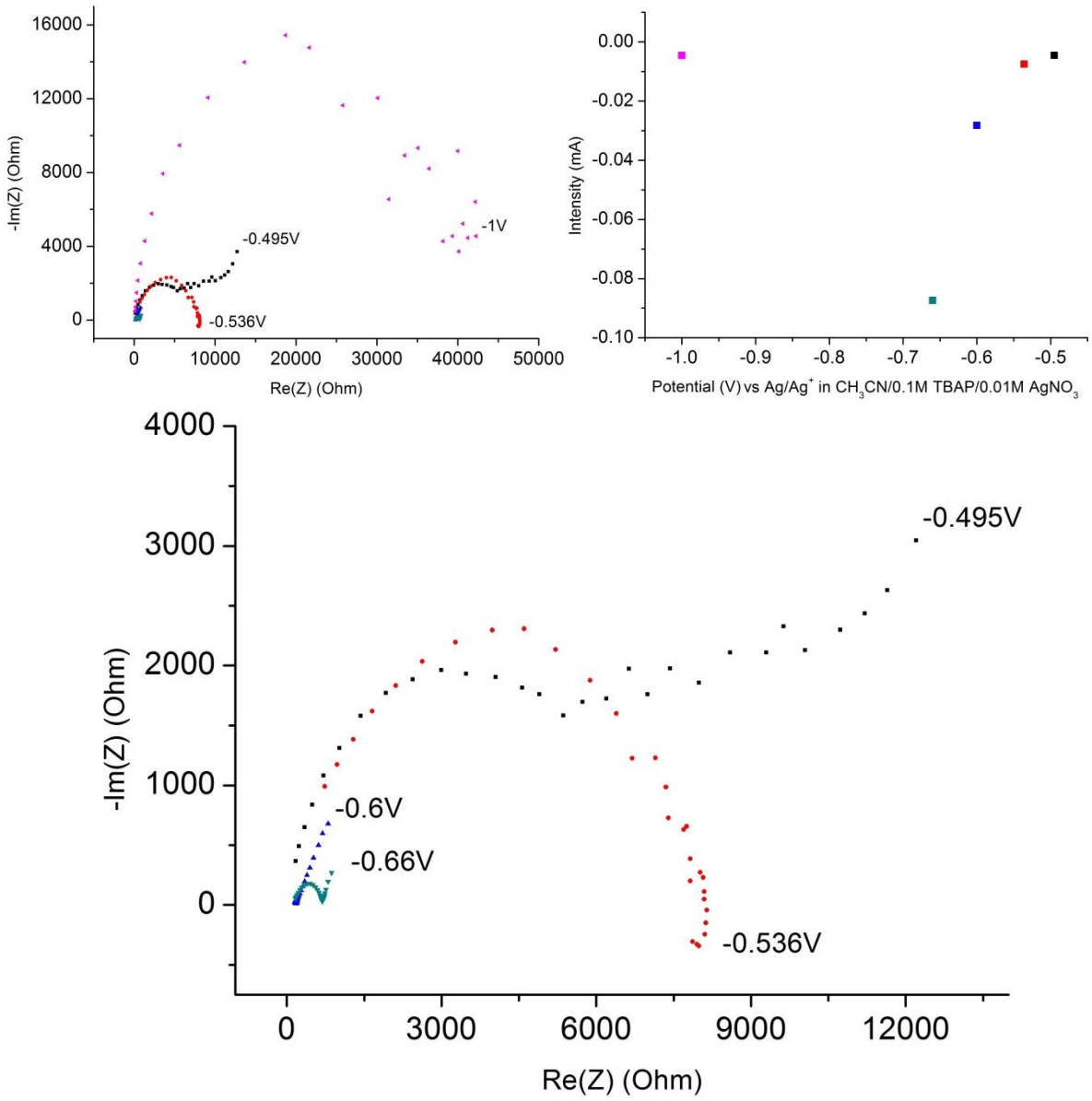


Fig. 6. Nyquist plot of the different potentials applied with Ar flux (second diagram is focus on the small impedance values) and it polarization curve.

In an attempt to identify and characterize the products growing and passivating the working electrodes, in situ spectroscopy analyses were carried out. Thus, UV-Vis spectra were recorded in real time using a transparent Indium Tin Oxide (ITO) working electrode as it was polarized to record a CV (Fig 7). The result is shown in figure 7b and clearly confirms the successive generation of two different products. The electrochemical signal of MBQ on the ITO electrode is worse than in glassy carbon electrode but still shows the two reduction peaks and the decrease of redox peaks upon cycling.

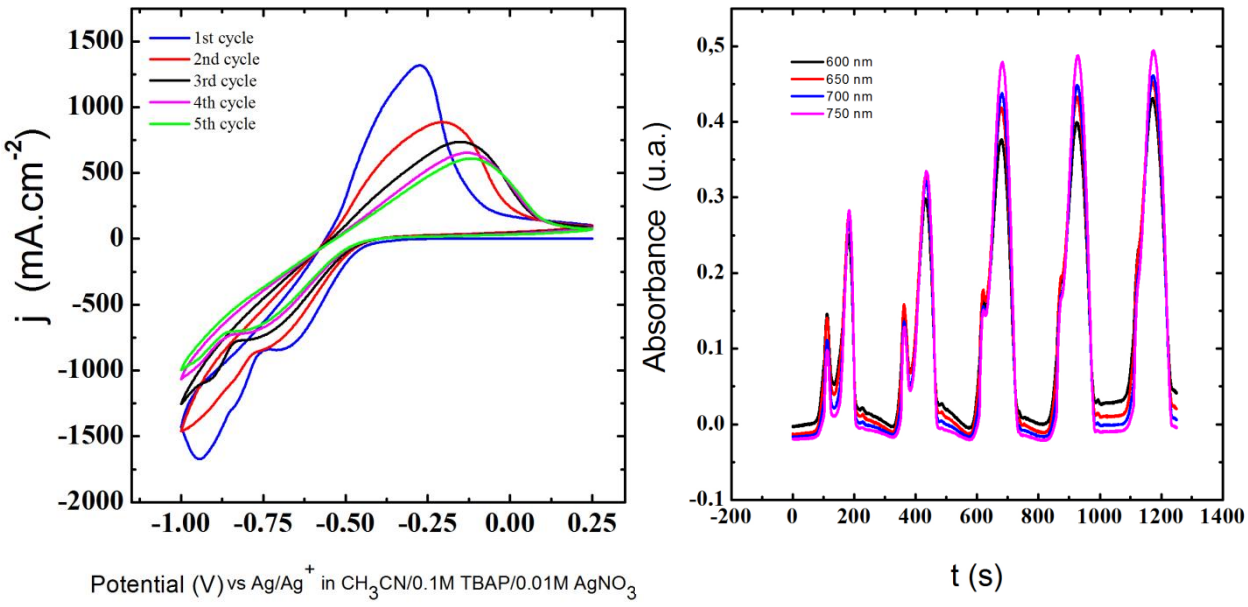


Fig. 7. Real time spectroscopy of an ITO working electrode at 10 mV $s^{-1}$ of 0.01M MBQ and 1.5M $LiClO_4$ in $CH_3CN$ solution (in air). (a) CVs of the first 5 cycles (b) Evolution of the absorbance at various visible wavelengths of the ITO working Electrode

Peaks in the absorbance spectra are produced when negative overpotentials were applied during the CV. In the first cycle of the CV can be clearly appreciated the generation and extinction of two different peaks in the absorbance spectra. This fit in with our hypothesis where a first product leads the generation of a second product by a polymerization process. Moving on next cycles of the CV the peaks of the absorbance spectra get closer until join together, in each cycle the amount of polymer on the electrode surface increase (due to the coating/polymerization processes are faster than it extinction by an oxidation process). Consequently after the oxidation still are polymer on the working electrode and in the next reduction step the first product is not able to be generated on the electrode surface because the polymer takes all the area of the working electrode. Therefore only is going to grow the polymer layer that is coating the electrode, so in the absorbance spectra only one peak appears.

So far we have been able to prove the electrochemical growth of the green coating (both in the presence and absence of oxygen) and the subsequent formation of passivating layers whose nature depends on the presence of oxygen. In order to determine whether these layers form exclusively through electrochemical processes we carried out an experiment consisting on the chemical reduction of solutions of MBQ in acetonitrile using metallic lithium as reducing agent.

Figure S2 includes a digital photograph showing the formation of the green layer on the surface of metallic lithium, thus proving that this compound can also be formed chemically as long as lithium is present. It should be noted that the green product grows on the surface of lithium but can be easily dispersed to the solution by

just a very gentle shaking. Remarkably, the final color of the solution was not green but orange, corresponding to the typical color of free reduced quinone anions, indicating the metastable nature of the green species. This result can contribute to an understanding of the structure of the green product, which must be formed by reduced quinone molecules with the implication of Li (the green layer was not formed in $TEA^+$ $TFB^-$ electrolytes).

With all the data at hand we propose the structure depicted in figure 8 (left structure), in which Li atoms bridge different reduced quinone molecules in an arrangement which is not purely ionic (only possible at reducing potentials) and only possible on the vicinity of the reducing electrode with a relatively large ratio of reduced quinone to lithium. The lack of covalent bonding between quinones would explain the low stability of this product, which upon stirring gets dissolved into the ($Li^+$ rich) bulk electrolyte solution yielding the red-orange reduced $Li_2$MBQ species.

A combined analysis of CV, PEIS and UV-Visible spectroscopy results allows us to propose a mechanism for the transformation (in air) of the green layer into a secondary product with an improved conductivity (shown by PEIS data) which eventually grows into a passivating coating on the surface of the WE. Starting from the green product (left structure), figure 8 shows the mechanism for further reduction. We relate the second reduction peak of the CV with a polymerization process, made possible by the catalytic reduction of $O_2$ by the green product[30,31] , a process obviously not possible in the absence of air. That process generates a polymer with a conductive structure that explains the reduction of the resistance on the PEIS experiments with respect to the initial green coating.

For experiments under Ar the green coating accumulates faster on the electrode thanks to the absence of $O_2$ that could otherwise oxidize part of the reduced MBQ. Thus, the polymerization process starts before, even at less negative potentials and there isn't a decrease of the current in the polarization curve between the MBQ redox and the polymerization processes. The final outcome is also a passivating layer. However, impedance data show that is not the same polymer obtained in air. Furthermore, the chaotic oscillation of current in the reduction area of the CV indicates that the electrode passivation doesn't follow a well-defined polymerization process as with $O_2$. In this case different reactions could take place, including Diels-Alder reaction or Michael addition[29]. A wide variety of structures could be generated in these processes, not only by reaction among quinone molecules but also possibly by heterogeneous reactions of quinones with the carbon electrode leading to covalent bonding. That fact could explain the widening oxidation peak and its shoulder in the CVs of deaerated solutions (figure 5) as well as the chaotic reduction currents. Unfortunately the wide possibilities for these processes do not allow for the proposal of a plausible mechanism in the absence of oxygen.

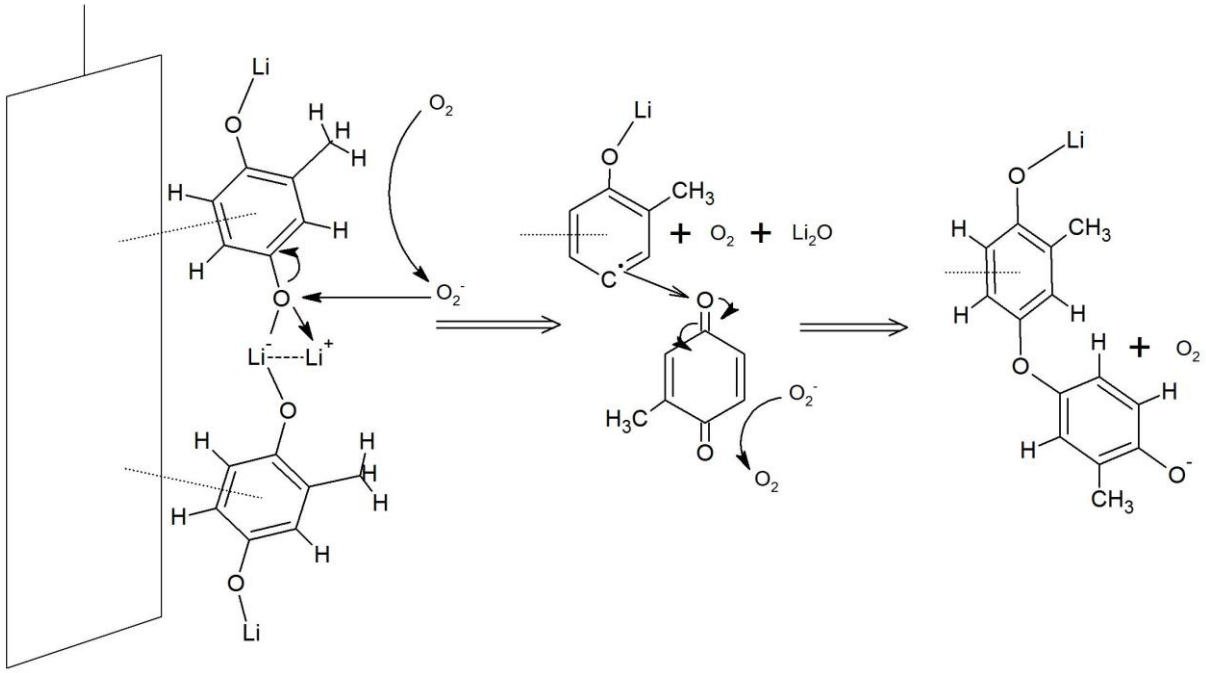


Fig. 8. Proposed mechanism for the MBQ polymerization process at ambient conditions.

The same kind of coating process described above was observed not only for MBQ but also for other quinones like p-benzoquinone (BQ) and 1,4-naphthoquinone (NQ). On the other hand the electrochemical reduction of anthraquinone (AQ) did not yield the green layer nor any passivating polymer. These facts reinforce our hypotheses because BQ and NQ could lead to polymerizations but anthraquinone would be too large and bulky and would present an important steric effect which would prevent the formation of structures like the ones depicted in figure 8. Due to this fact CVs of AQ doesn't show a decrease in the intensity with the cycles at any scan rate and the second reduction peak related with the polymerization process, figure S3. On the other hand CV of BQ show even at 100 mV $s^{-1}$ a decrease in the intensity with the cycles and the second reduction peak related with the polymerization process which generates new and more complex spices, figure S4, consequently the redox profile is more complex than the AQ redox profile.

~~On the other hand, p-benzoquinone with its minimal steric hindrance showed a decrease of the intensity in each cycle on the CVs even at 100 mV $s^{-1}$ (figure S3) indicating the fastest generation of this type of polymeric structures among the quinones studied.~~

## Conclusions

The possible use of quinones in organic lithium electrolytes for application in Redox Flow Batteries could benefit from wider stability windows and higher solubility in organic media. However, a high concentration of quinones on the electrode-

electrolyte interphase is precisely one of the conditions leading to the type of passivating coatings that we have reported here.

Our results show the large influence of $Li^+$ on the MBQ redox mechanism, showing mainly a couple of redox peaks and increasing the electrochemical reversibility of the MBQ redox process.

On the other hand, we have proven the systematic and reversible generation of a green coating that increases the resistance of the electrode and prevents the regular redox process of MBQ to take place, regardless of the presence of $O_2$ in solution and the nature of the electrode material. We have proven the involvement of Li in the formation of this green coating by showing its growth by chemical reduction with Li metal in $CH_3CN$ and its absence when other electrolytes such as $TEA^+$ $TFB^-$ were used. That green product is not stable and easily disassembles into individual reduced Li-MBQ molecules. We have also shown the generation of new and different products on this first coating that increase notably the resistance of the electrode, and which nature depends on the presence or absence of $O_2$. All of these coatings have a detrimental effect for the use of quinones in organic electrolytes. On the other hand, we have found that larger quinones such as anthraquinone can be reversibly cycled without formation of the passivating layers, whereas quinones with no steric impediments quickly yield these coatings on the current collector.

Thus, our work allows us to conclude that in order to apply quinones for energy storage in RFBs making use of organic media, two main guidelines should be considered. Large, sterically hindered quinones should be used instead of simpler quinones prone to polymerization in the presence of $Li^+$. Otherwise, organic electrolytes not containing $Li^+$ would be preferable.

Despite the hurdles found in our research, the use of organic quinone electrolytes still presents strong advantages which could be put to work in their application in RFBs. We hope that the work reported here will help in preventing some of the drawbacks of these systems, thus contributing to setting the path for organic quinone electrolytes to be applied in redox flow batteries.

## Acknowledgements

Partial funding from Miisterio de Economía y Competitividad through Fondo Europeo de Desarrollo Regional (FEDER) (Grant MAT2015-68394-R, MINECO/FEDER) is acknowledged. ICN2 acknowledges support of the Spanish MINECO through the Severo Ochoa Centers of Excellence Program under Grant SEV-2013-0295. Finally, the award to

DPD of a Marie-Curie Fellowship through Beatriu de Pinos Program (BP-DGR-2013) from the Catalan system of science and technology, Spain, is gratefully acknowledged.

Special thanks to Prof. Fritz Huguenin and Wellington J. A. S. Gomes, (Departamento de Química, Faculdade de Filosofia, Ciências e Letras de Ribeirão Preto−Universidade de São Paulo) for the UV-Vis experiments.

## References

1. Guin, P. S., Das, S. & Mandal, P. C. Electrochemical Reduction of Quinones in Different Media: A Review. *Int. J. Electrochem.* **2011,** 1–22 (2011).
2. Chen, Q., Eisenach, L. & Aziz, M. J. Cycling Analysis of a Quinone-Bromide Redox Flow Battery. *J. Electrochem. Soc.* **163,** A5057–A5063 (2016).
3. Huskinson, B. *et al.* A metal-free organic-inorganic aqueous flow battery. *Nature* **505,** 195–8 (2014).
4. Quan, M., Sanchez, D., Wasylkiw, M. F. & Smith, D. K. Voltammetry of Quinones in Unbuffered Aqueous Solution: Reassessing the Roles of Proton Transfer and Hydrogen Bonding in the Aqueous Electrochemistry of Quinones. *J. Am. Chem. Soc.* **129,** 12847–12856 (2007).
5. Alizadeh, K. & Shamsipur, M. Calculation of the two-step reduction potentials of some quinones in acetonitrile. *J. Mol. Struct. THEOCHEM* **862,** 39–43 (2008).
6. Gupta, N. & Linschitz, H. Hydrogen-bonding and protonation effects in electrochemistry of quinones in aprotic solvents. *J. Am. Chem. Soc.* **119,** 6384–6391 (1997).
7. Tonholo, J. *et al.* Electrochemical properties of biologically active heterocyclic naphthoquinones. *J. Braz. Chem. Soc.* **9,** 163–169 (1998).
8. Macías-Ruvalcaba, N. a., González, I. & Aguilar-Martínez, M. Evolution from Hydrogen Bond to Proton Transfer Pathways in the Electroreduction of α-NH-Quinones in Acetonitrile. *J. Electrochem. Soc.* **151,** E110 (2004).
9. Alligrant, T. M. & Alvarez, J. C. The Role of Intermolecular Hydrogen Bonding and Proton Transfer in Proton-Coupled Electron Transfer. *J. Phys. Chem. C* **115,** 10797–10805 (2011).
10. Alligrant, T. M., Hackett, J. C. & Alvarez, J. C. Acid/base and hydrogen bonding effects on the proton-coupled electron transfer of quinones and hydroquinones in acetonitrile: Mechanistic investigation by voltammetry, 1H NMR and computation. *Electrochim. Acta* **55,** 6507–6516 (2010).

11. Nikitina, V. a., Nazmutdinov, R. R. & Tsirlina, G. a. Quinones electrochemistry in room-temperature ionic liquids. *J. Phys. Chem. B* **115,** 668–677 (2011).

12. Guin, P. S., Das, S. & Mandal, P. C. Electrochemical reduction of sodium 1,4-dihydroxy-9,10- anthraquinone-2-sulphonate in aqueous and aqueous dimethyl formamide mixed solvent: A cyclic voltammetric study. *Int. J. Electrochem. Sci.* **3,** 1016–1028 (2008).

13. Electroanal, J., Russel, C. & Jaenicke, W. Heterogeneous electron exchange of quinones in aprotic solvents, part III. *Electroanalysis* **199,** 139–151 (1986).

14. Bao, D. *et al.* Electrochemical reduction of quinones: Interfacing experiment and theory for defining effective radii of redox moieties. *J. Phys. Chem. B* **114,** 14467–14479 (2010).

15. Seto, K., Nakayama, T. & Uno, B. Formal redox potentials of organic molecules in ionic liquids on the basis of quaternary nitrogen cations as adiabatic electron affinities. *J. Phys. Chem. B* **117,** 10834–10845 (2013).

16. T.Fujinaga, K.Izutsu, T. N. Efect of metal ions on the polarographic reduction of organic compounds in dipolar aprotic solvents. *Electroanal. Chem. INTERFACIAL Electrochem. Elsevier Sequoia S.A., Lausann* **29,** 203–209 (1971).

17. Choi, D. *et al.* Electrochemical recognition of ammonium and alkali metal cations with calix[4]arenediquinone. *J. Electroanal. Chem.* **387,** 133–134 (1995).

18. Cheng, W. X. *et al.* Investigation on the π-dimer/σ-dimer of 1,8-dihydroxy-9,10-anthracenedione in the process of electrochemical reduction by using IR spectroelectrochemical cyclic voltabsorptometry and derivative cyclic voltabsorptometry. *J. Phys. Chem. C* **117,** 3940–3948 (2013).

19. Li, D., Cheng, L. & Jin, B. Investigation on PCET-accompanied Dimerization of 5-hydroxy-1, 4-naphthoquinone in the Process of Electrochemical Reduction by in Situ FT-IR Spectroelectrochemistry and Density Functional Calculation. *Electrochim. Acta* **130,** 387–396 (2014).

20. Macías-Ruvalcaba, N. A. & Evans, D. H. Association reactions of the anion radicals of some hydroxyquinones: Evidence for formation of π- And σ-dimers as well as a neutral-anion radical complex. *J. Phys. Chem. C* **114,** 1285–1292 (2010).

21. Rieke, R. D., Saji, T. & Kujundzic, N. Vo ltammetric measurements Electrochemical synthesis of diduroquinone. **102,** 397–405 (1979).

22. Algharaibeh, Z. & Pickup, P. G. Charge trapping in poly(1-amino-anthraquinone) films. *Electrochim. Acta* **93,** 87–92 (2013).

23. Balasubramaniam, E. *et al.* Electrochemical Preparation of Anthraquinone and Zinc Porphyrin Coated Electrodes - Redox Activity and Film Stability. *J. Mater. Chem.* **5,** 625–629 (1995).

24. Yamamoto, T. & Etori, H. Poly(anthraquinone)s Having a π-Conjugation

System along the Main Chain. Synthesis by Organometallic Polycondensation, Redox Behavior, and Optical Properties. *Macromolecules* **28,** 3371–3379 (1995).

25. Suematsu, S. & Naoi, K. Quinone-introduced oligomeric supramolecule for supercapacitor. *J. Power Sources* **97-98,** 816–818 (2001).

26. Naoi, K., Suematsu, S., Hanada, M. & Hideaki, T. Enhanced Cyclability of π-π Stacked Supramolecular (1,5-Diaminoanthraquinone) Oligomer as an Electrochemical Capacitor Material. *J. Electrochem. Soc.* **149,** A472 (2002).

27. Naoi, K., Suematsu, S. & Manago, A. Electrochemistry of poly(1,5-diaminoanthraquinone) and its application in electrochemical capacitor materials. *J. Electrochem. Soc.* **147,** 420–426 (2000).

28. Gao, M., Yang, F., Zhang, G., Liu, L. & Wang, X. Effects of poly-1,5-diaminoanthraquinone morphology on oxygen reduction in acidic solution. *Electrochim. Acta* **54,** 2224–2228 (2009).

29. Dongmo, S., Witt, J. & Wittstock, G. Electropolymerization of quinone-polymers onto grafted quinone monolayers: A route towards non-passivating, catalytically active film. *Electrochim. Acta* **155,** 474–482 (2015).

30. Newton, L. a. a., Cowham, E., Sharp, D., Leslie, R. & Davis, J. Plumbagin: a natural product for smart materials? *New J. Chem.* **34,** 395 (2010).

31. Ardakani, M. M., Karami, P. E., Zare, H. R. & Hamzehloo, M. Electrocatalytic reduction of oxygen on the surface of glassy carbon electrodes modified with plumbagin. *Microchim. Acta* **159,** 165–173 (2007).